AD NUMBER: AD0846250
LIMITATION CHANGES
TO: Approved for public release; distribution is unlimited.
FROM: Distribution authorized to US Government Agencies and their Contractors; Export Control; 1 Dec 1968. Other requests shall be referred to Army Missile Command, Redstone Arsenal, AL, 35809.
AUTHORITY
USAMC ltr dtd 23 Aug 1971

REPORT NO. RS-TR-68-15

NUMERICAL METHODS FOR THE NONLINEAR ANALYSIS OF AN ELASTIC ARCH

by

Grady E. Patrick, Jr.

December 1968

This document is subject to special export controls and each transmittal to foreign governments or foreign nationals may be made only with prior approval of this Command, ATTN: AMSMI-RS.

U.S. ARMY MISSILE COMMAND

Redstone Arsenal, Alabama

DISPOSITION INSTRUCTIONS

Destroy this report when it is no longer needed. Do not return it to the originator.

DISCLAIMER

The findings in this report are not to be construed as an official Department of the Army position unless so designated by other authorized documents.

9 December 1968

Report No. RS-TR-68-15

NUMERICAL METHODS FOR THE NONLINEAR ANALYSIS OF AN ELASTIC ARCH

by

Grody E. Patrick, Jr.

DA Project No. 1L013001A91A
AMC Management Structure Code No. 5016.11.84400.60

This document is subject to special export controls and each transmittal to foreign governments or foreign nationals may be made only with prior approval of this Command, ATTN: AMSMI-RS.

Stress and Thermodynamics Analysis Branch
Structures and Mechanics Laboratory
Research and Development Directorate
U. S. Army Missile Command
Redstone Arsenal, Alabama 35809

ABSTRACT

In a recent paper, Wempner presented a method by which the finite deflections of thin shells are approximated in finite elements and the nonlinear differential equations are replaced by nonlinear algebraic equations. This is accomplished by decomposing the motion of an element into a rigid-body rotation and a deformation. The deformation of a Hookean element is characterized by linear constitutive equations relating generalized forces and small relative displacements. Nonlinearities arise from the differences in the rigid-body rotations of adjacent elements.

In the present paper, the method is applied to formulate algebraic equations for the finite deflections of a circular arch. The constitutive equations of the finite element are the exact linear equations of the Winkler-Bach theory.

The nonlinear algebraic equations are replaced by a succession of linear equations, each governing the response to a small increment of load. To eliminate cumulative error, the numerical results are inserted in the nonlinear equations and corrected by the Newton-Raphson procedure.

ACKNOWLEDGEMENTS

The author wishes to express sincere thanks to Dr. G. A. Wempner, Dr. J. T. Oden, and Dr. R. R. Reed of the University of Alabama, Huntsville, for their helpful suggestions in the preparation of this work.

In addition, the author wishes to thank Mr. T. A. Smith and Mr. J. R. Sandlin for their advice.

CONTENTS

ILLUSTRATIONS

SYMBOLS

A	cross-sectional area
E	Young's modulus
F_N	external shear acting on element N
M_N	moment on element N
N_N	tension force on element N
P_N	external normal load acting on element N
Q_N	shear force on element N
R	radius to center line
ΔU_N	small tangential displacement of element N
ΔV_N	small radial displacement of element N
Z	property of cross section, defined by eq. (12)
$\Delta\beta_N$	relative rotation of the ends of element N
γ	strain energy, defined by eq. (16)
ρ	angle of incidence of the applied load
ϕ_N	sum of $\Delta\phi_N$ to the element N
$\Delta\phi_N$	angle subtended by arc N

Subscripts

N	signifies element numbered N
cr	critical load

CHAPTER I

INTRODUCTION

Classically, the analysis of continuous systems begins with investigations of the properties of small differential elements of the continuum under investigation. Relationships are established between mean values of various quantities associated with the infinitesimal elements, and partial differential equations or integral equations governing the behavior of the entire domain are obtained by allowing the dimensions of the element to approach zero as the number of elements becomes infinitely large.

The resulting equations are often nonlinear, even for relatively simple geometries, and one must resort to a numerical procedure to obtain quantitative solutions to the nonlinear problem. Regardless of the initial assumptions and the methods used to formulate a nonlinear problem in solid mechanics, if numerical methods are employed to evaluate the results, the continuum is essentially approximated by a discrete model.

Discrete models for nonlinear analysis of flexible shells are described by Oden and Wempner [1]. The methods are based upon the use of finite elements for approximations of the continuous body. The equations describing the continuum may be employed to arrive at the properties of these elements, but the dimensions of the elements remain finite in the analysis, integrations are replaced by finite summations, and the partial differential equations of the continuous media are replaced by systems of algebraic or ordinary differential equations. The continuum with infinitely many degrees of freedom is thus represented by a discrete model which has finite degrees of freedom.

Large deflections are treated by decomposing the motion of the element into a rigid-body motion followed by a deformation. The decomposition has the effect of extending many existing formulations for linearly elastic elements to problems involving geometrical nonlinearities, particularly finite rotations and buckling.

The methods are applied here to the particular problem of a circular arch subjected to a concentrated load applied at the crown as depicted in Figures 1 and 2.

As the load P is increased, the deflection δ will follow the symmetrical path (0 - 1) as indicated in Figure 2. When the load reaches a value corresponding to the branch point (1), the arch can assume unsymmetical configurations represented by curves (1 - 3) and (1 - 4) or the arch may follow a symmetrical path (1 - 5).

In the discrete representation of the arch, the path (0 - 1) is obtained by incrementing the load and computing the corresponding displacements. The branch point is signaled by the vanishing of the determinant of a coefficient matrix. At the branch point, the coefficient matrix must be rearranged so as to permit a solution for the load increment corresponding to a

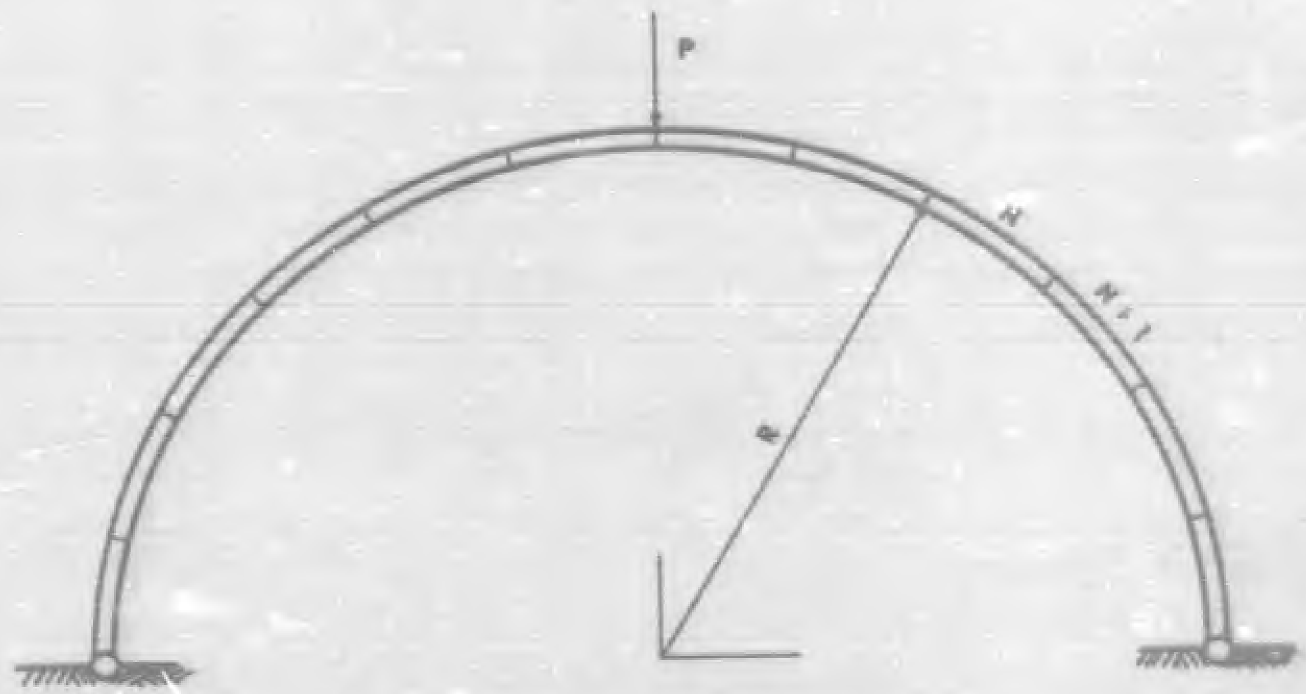

Figure 1. Circular Arch

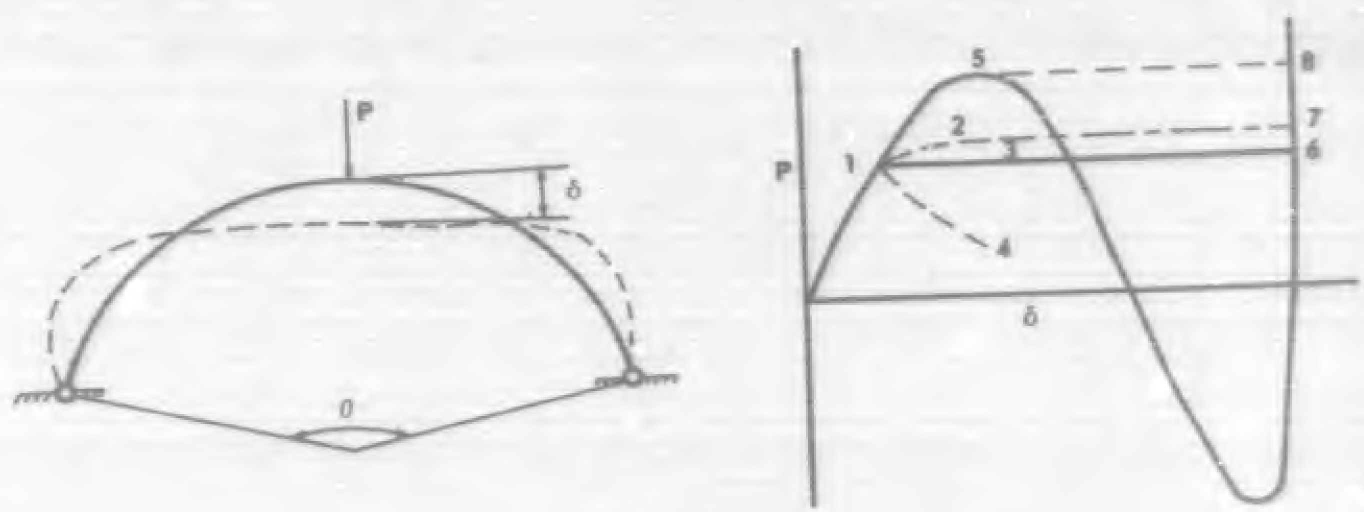

Figure 2. Deflection

prescribed increment in vertical displacement. Incrementing the displacement will produce one of the following three results:

1. If the load decreases with increase in displacement, the path will be the lower unstable curve (1 - 4). However, inasmuch as this point is not physically attainable by the arch unless restrained, the arch will snap through to point (6).
2. If the load increases with increase in displacement and side sway is also present, the path will be (1 - 3). When point (2) is reached, snap through will occur to point (7).
3. Finally, if the arch follows a symmetric deformation, the load increases with displacement and the path traced will be that of (1 - 5 - 8).

CHAPTER II

PROBLEM FORMULATION

The continuous arch is subdivided into small finite elements. The angle subtended by the element N is $\Delta\phi_N$ and the radius of the centerline is R, as shown in Figure 3. The thickness is h and the width b. The elements lying in the first quadrant are identified by a subscript (+), and the elements lying in the second quadrant are identified by a subscript (-). Since all elements are the same[1] (Figure 4) we need only derive the kinematical, constitutive, and equilibrium equations for the arbitrary element.

The elements are assumed small enough so that relative displacements are small within an element, and, therefore, linear (classical) methods are adequate for the derivation of the constitutive equations only. The normals to the elements before and after deformation are $\hat{a}_N$ and $\hat{A}_N$ and the rotation of these normals is β_N.

---

[1]Symmetric deformation shown, but deformation need not be symmetric

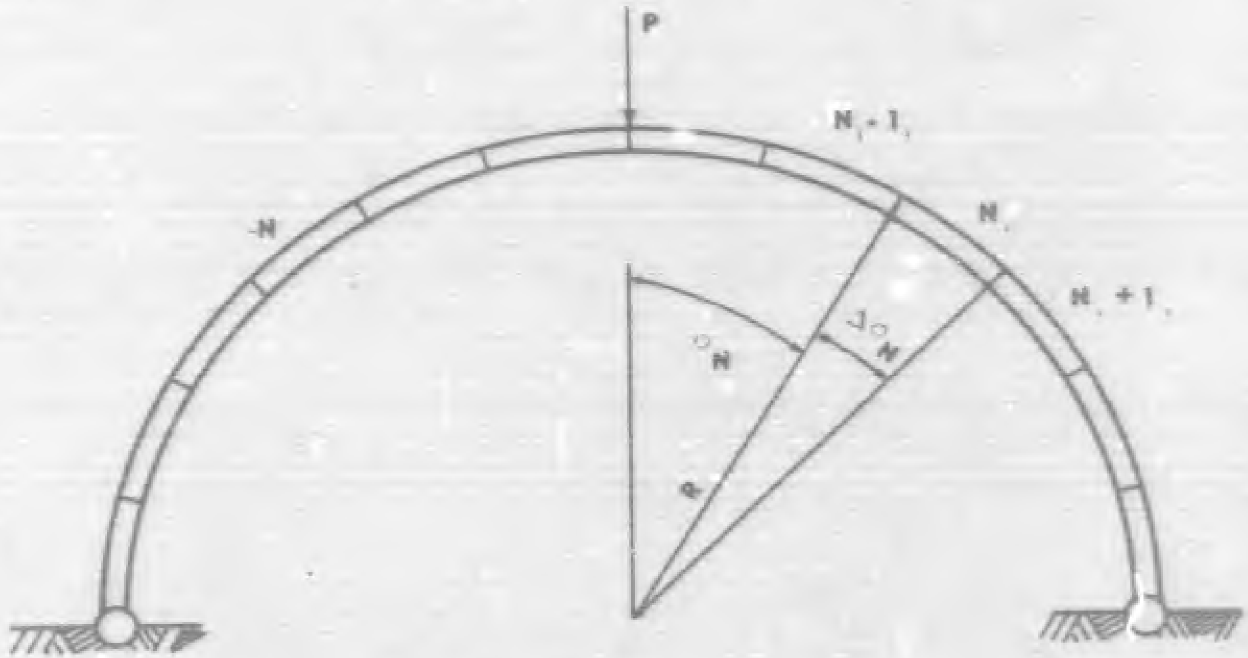

Figure 3. The Subdivided Arch

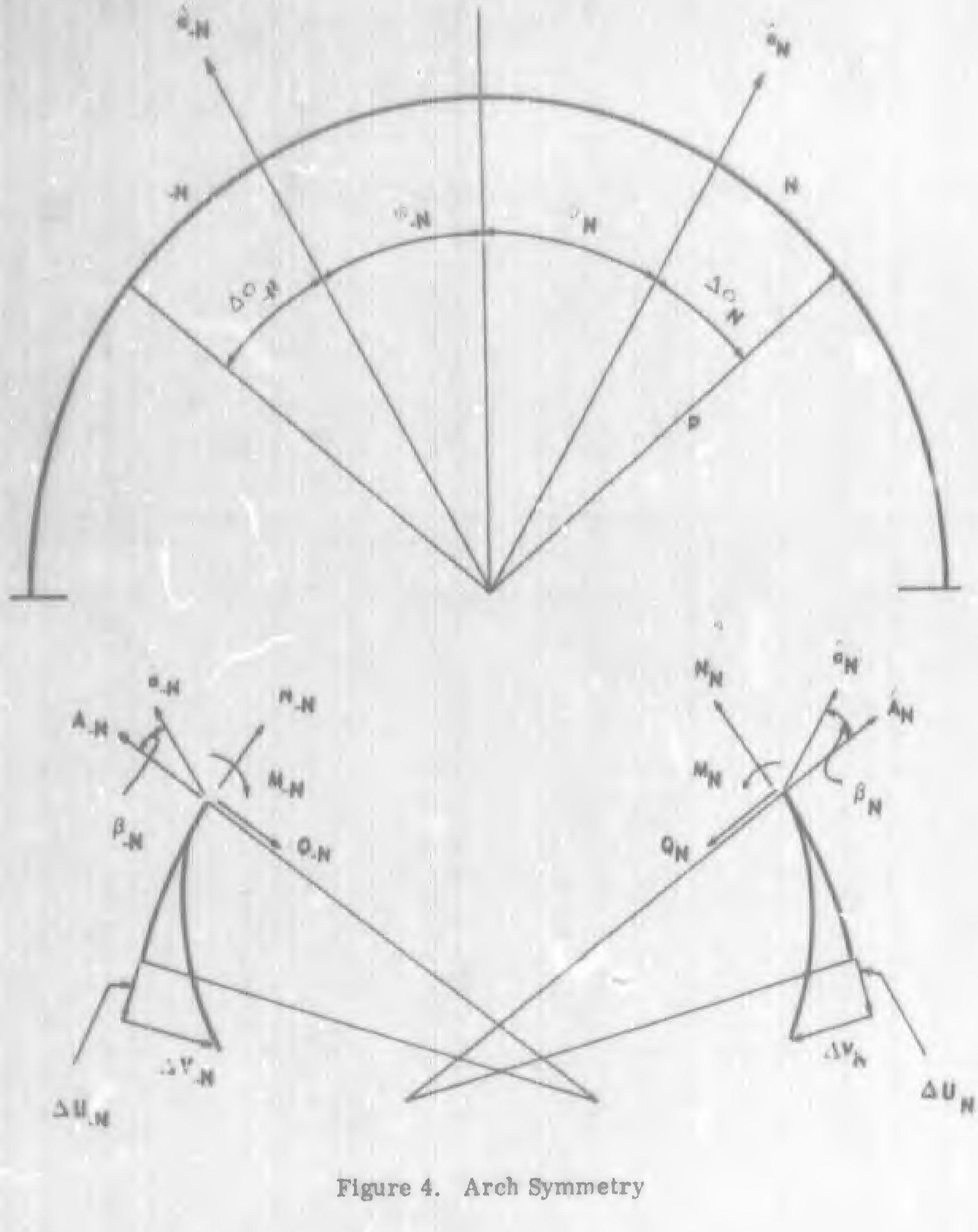

Figure 4. Arch Symmetry

A. Kinematical Equations

The work done by Toupin [2] has shown that the motion of a continuous medium in the neighborhood of a particle can be decomposed into a rigid body motion followed by a deformation or vice-versa. If we assume that the finite element is small enough to provide a valid representation for the discrete system, then the motion of the small finite element can be decomposed in the manner of Toupin's analysis. On this basis, we examine the small relative displacements and relative rotations which determine the small strains within the element.

Consider the element N as shown in Figure 5 which has end points I and J in the undeformed state. It is then rigidly transported to I', J' and then given a small relative displacement to I*, J*, the point I' and I* being the same. Thus, the motion of the element consists of three parts: (a) a translation, (b) a rotation, and (c) a deformation.

The vector $\vec{p}$ determines the magnitude and direction of the chord of the element N before deformation as shown in Figure 6.

$$\vec{p} = 2R \sin\left(\frac{\Delta\phi_N}{2}\right)\left[\pm\hat{i} \cos\left(\phi_N + \frac{\Delta\phi_N}{2}\right) - \hat{j} \sin\left(\phi_N + \frac{\Delta\phi_N}{2}\right)\right] \tag{1}$$

The vector $\vec{p}$ remains unchanged in magnitude as the element is rigidly transported to I', J', but due to the rigid body rotation β_N the magnitude and direction are now determined by

$$\vec{p}' = 2R \sin\left(\frac{\Delta\phi_N}{2}\right)\left[\pm\hat{i} \cos\left(\phi_N + \beta_N + \frac{\Delta\phi_N}{2}\right) - \hat{j} \sin\left(\phi_N + \beta_N + \frac{\Delta\phi_N}{2}\right)\right]. \tag{2}$$

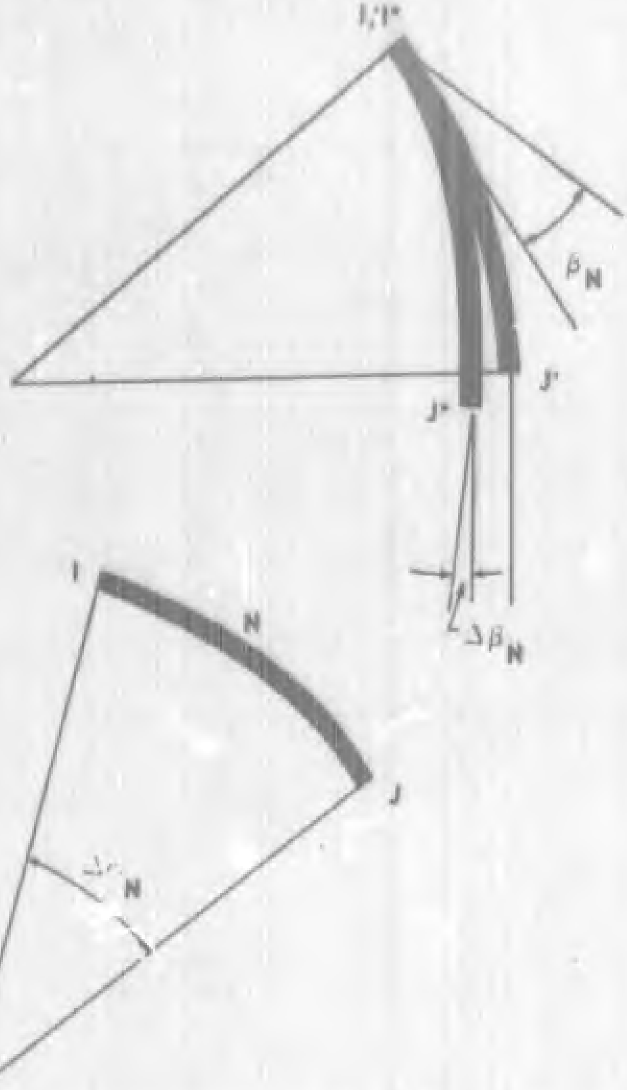

Figure 5. Decomposition of the Motion of the Element

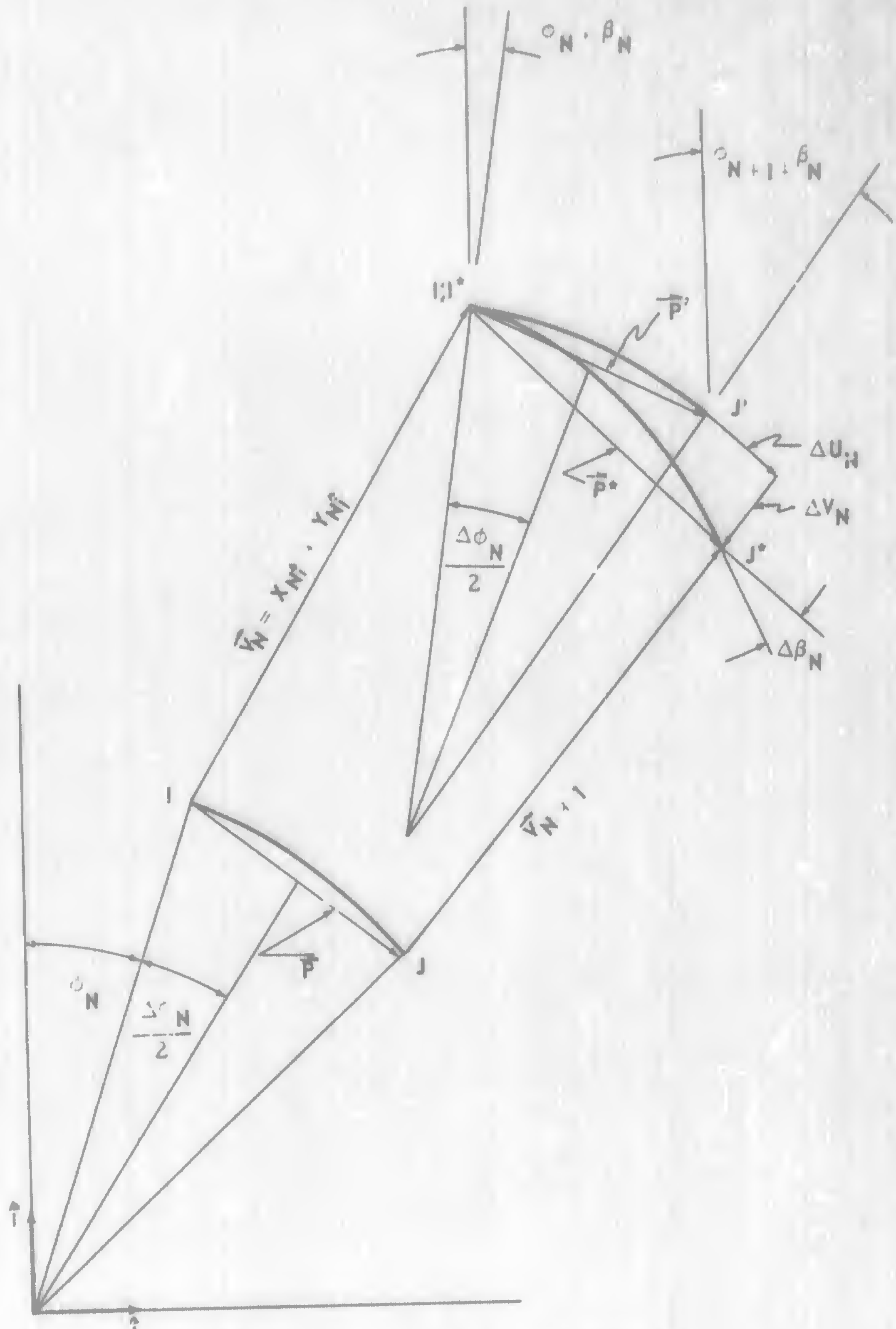

Figure 6. Kinematics of the Element

The motion of the element N from I', J' to I*, J* involves a relative rotation $\Delta\beta_N$, a small tangential displacement ΔU_N, and a small radial displacement ΔV_N of the right end relative to the left end. These motions $\Delta\beta_N$, ΔU_N, and ΔV_N are assumed small to justify linear analysis. Due to these motions, the magnitude and direction of the element chord is

$$\vec{p^*} = \vec{p'} \pm \left[\Delta U_N \cos\left(\phi_{N+1} + \beta_N\right) - \Delta V_N \sin\left(\phi_{N+1} + \beta_N\right)\right] \hat{i} - \left[\Delta U_N \sin\left(\phi_{N+1} + \beta_N\right) + \Delta V_N \cos\left(\phi_{N+1} + \beta_N\right)\right] \hat{j} . \tag{3}$$

The displacement of point I as it goes to I* is

$$\vec{V}_N = X_N \hat{i} + Y_N \hat{j} \tag{4}$$

and that of J to J*

$$\vec{V}_{N+1} = X_{N+1} \hat{i} + Y_{N+1} \hat{j} . \tag{5}$$

Thus, the displacement of J* relative to I* is

$$\vec{V}_{N+1} - \vec{V}_N = \Delta X_N \hat{i} + \Delta Y_N \hat{j} = \Delta\vec{V}_N \tag{6}$$

or

$$\Delta\vec{V}_N = \vec{p^*} - \vec{p} . \tag{7}$$

Let

$$\phi_{N1/2} = \phi_N + \frac{\Delta\phi_N}{2} \tag{8}$$

and with the aid of eq. (1), (2), and (3), eq. (7) becomes

$$\vec{\Delta V}_N = \pm \hat{i} \left\{ \Delta U_N \cos\left(\phi_{N+1} + \beta_N\right) - \Delta V_N \sin\left(\phi_{N+1} + \beta_N\right) + 2R \sin\left(\frac{\Delta\phi_N}{2}\right)\left[\cos\left(\phi_{N1/2} + \beta_N\right) - \cos\left(\phi_{N1/2}\right)\right]\right\} - \hat{j}\left\{\Delta U_N \sin\left(\phi_{N+1} + \beta_N\right) + \Delta V_N \cos\left(\phi_{N+1} + \beta_N\right) + 2R \sin\left(\frac{\Delta\phi_N}{2}\right)\left[\sin\left(\phi_{N1/2} + \beta_N\right) - \sin\left(\phi_{N1/2}\right)\right]\right\}. \tag{9}$$

By eq. (6)

$$\Delta X_N = \pm \left\{ \Delta U_N \cos\left(\phi_{N+1} + \beta_N\right) - \Delta V_N \sin\left(\phi_{N+1} + \beta_N\right) + 2R \sin\left(\frac{\Delta\phi_N}{2}\right)\left[\cos\left(\phi_{N1/2} + \beta_N\right) - \cos\left(\phi_{N1/2}\right)\right]\right\} \tag{10a}$$

$$\Delta Y_N = - \left\{ \Delta U_N \sin\left(\phi_{N+1} + \beta_N\right) + \Delta V_N \cos\left(\phi_{N+1} + \beta_N\right) + 2R \sin\left(\frac{\Delta\phi_N}{2}\right)\left[\sin\left(\phi_{N1/2} + \beta_N\right) - \sin\left(\phi_{N1/2}\right)\right]\right\} \tag{10b}$$

B. Equilibrium Equations

1. Equilibrium of the Element. To be consistent with the assumptions of linear behavior, we neglect the deformations in the derivation of the equilibrium equations for the element. The equilibrium equations are easily derived as follows:

The forces shown in Figure 7 acting on element N are N_N, Q_N, and M_N, the tensile, shear, and moment, respectively, acting at the left end of the element and N'_N, Q'_N, and M'_N at the right end.

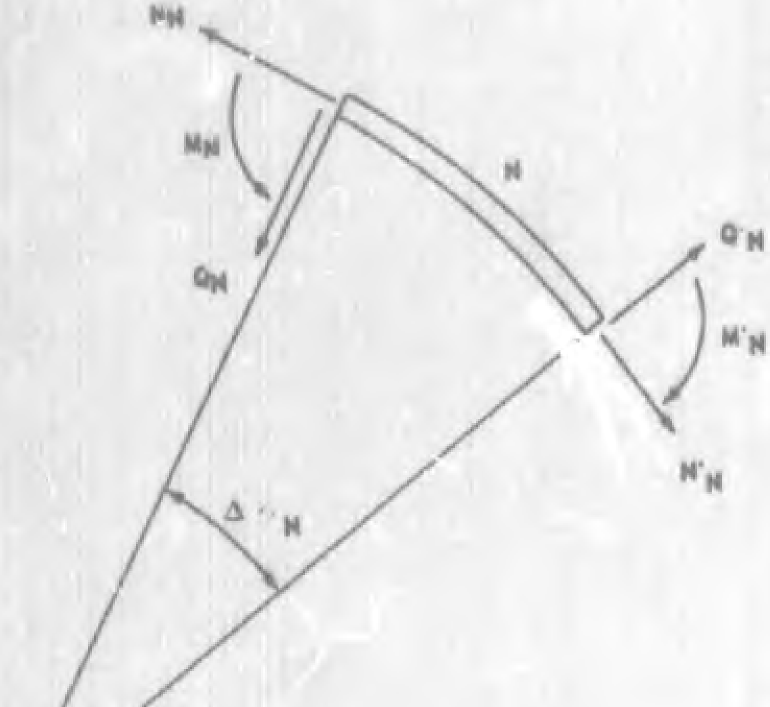

Figure 7. Equilibrium of the Element

Since it is convenient to formulate the problem in nondimensional quantities, we define the following terms:

$$n_N \equiv \frac{N_N}{EAZ} \tag{11a}$$

$$m_N \equiv \frac{M_N}{REAZ} \tag{11b}$$

$$q_N \equiv \frac{Q_N}{EAZ} \tag{11c}$$

$$p_N \equiv \frac{P_N}{EAZ} \text{ ; external radial loads} \tag{11d}$$

$$f_N \equiv \frac{F_N}{EAZ} \text{ ; external shear forces} \tag{11e}$$

where N_N, Q_N, M_N are the forces acting at the left end of the element, E is Young's modulus, A is the cross-sectional area, R is the radius of the centroid of the element, and Z is a property of the cross section and is defined as

$$Z = \frac{1}{AR} \iint \frac{z^2}{R + z}\, dA \tag{12}$$

where z is a radial distance from the centroid of the element.

We obtain from Figure 7 and by the use of the nondimensional quantities of eq. (11) and the three equations of equilibrium:

$$n'_N = n_N \cos \Delta\phi_N - q_N \sin \Delta\phi_N \tag{13a}$$

$$q'_N = q_N \cos \Delta\phi_N + n_N \sin \Delta\phi_N \tag{13b}$$

$$m'_N = m_N + n_N (1 - \cos \Delta\phi_N) + q_N \sin \Delta\phi_N \tag{13c}$$

These are linear equations which relate the forces and moments on the right end of element N to those forces and moments on the left end of the element.

2. Joint Equilibrium. In the derivation of the equilibrium equations, the displacements and rotations of the element were neglected. However, when two adjoining elements, N and N + 1, are brought together to form the continuous arch, a normal $\hat{a}_N$ at the right end of element N is not colinear after deformation with the normal $\hat{a}_{N+1}$ at the left end of element N + 1 but differ by the amount of the relative rotation $\Delta\beta_N$ of element N. This is depicted in Figure 8.

The forces at the right end of element N are N'_N, Q'_N and M'_N and those forces at the left end of element N + 1 are N_{N+1}, Q_{N+1}, and M_{N+1}. By considering rotation $\Delta\beta_N$, the nondimensional relations given by eq. (11), and from Figure 9, the following relationships between the forces on the right end of the element N and the forces on the left end of element N + 1 can be obtained:

$$n_{N+1} = - f_{N+1} + n'_N - q'_N \Delta\beta_N \tag{14a}$$

$$q_{N+1} = - p_{N+1} + q'_N + n'_N \Delta\beta_N \tag{14b}$$

$$m_{N+1} = m'_N \tag{14c}$$

It should be noted that the eq. (14) are nonlinear since we have products of forces and rotations occurring in these relations.

If there are no external loads acting on the joint, the terms f_{N+1} and p_{N+1} become zero.

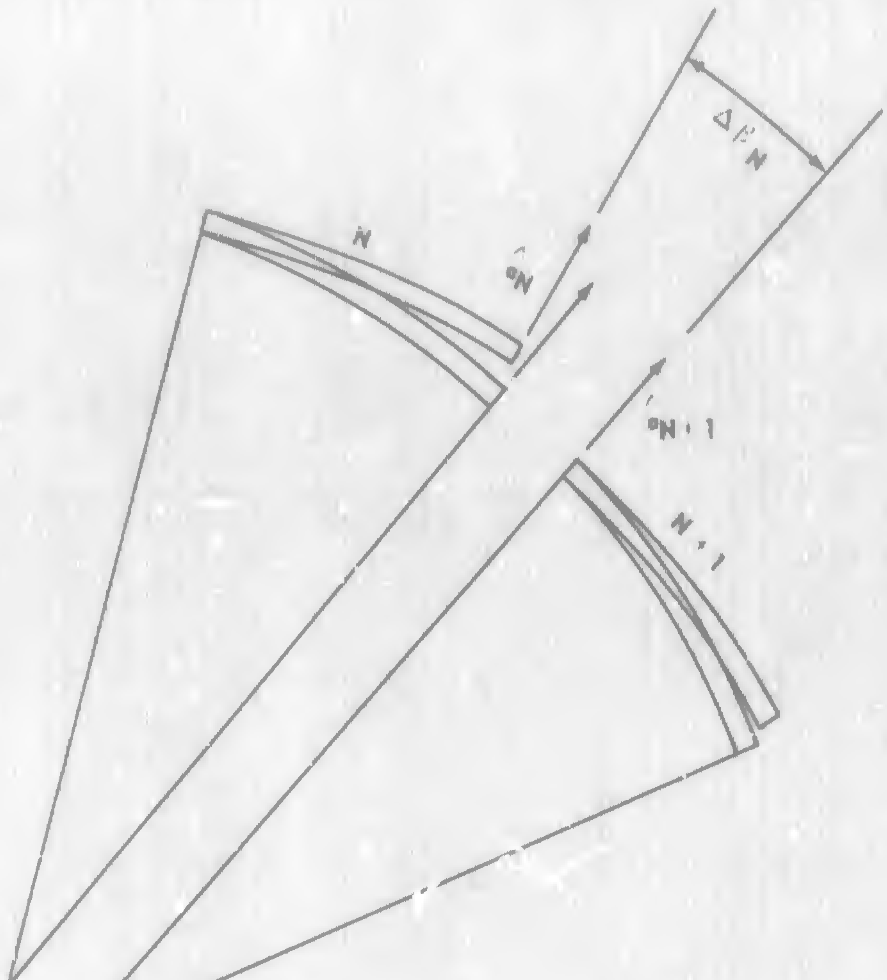

Figure 8. Rotation of Normals

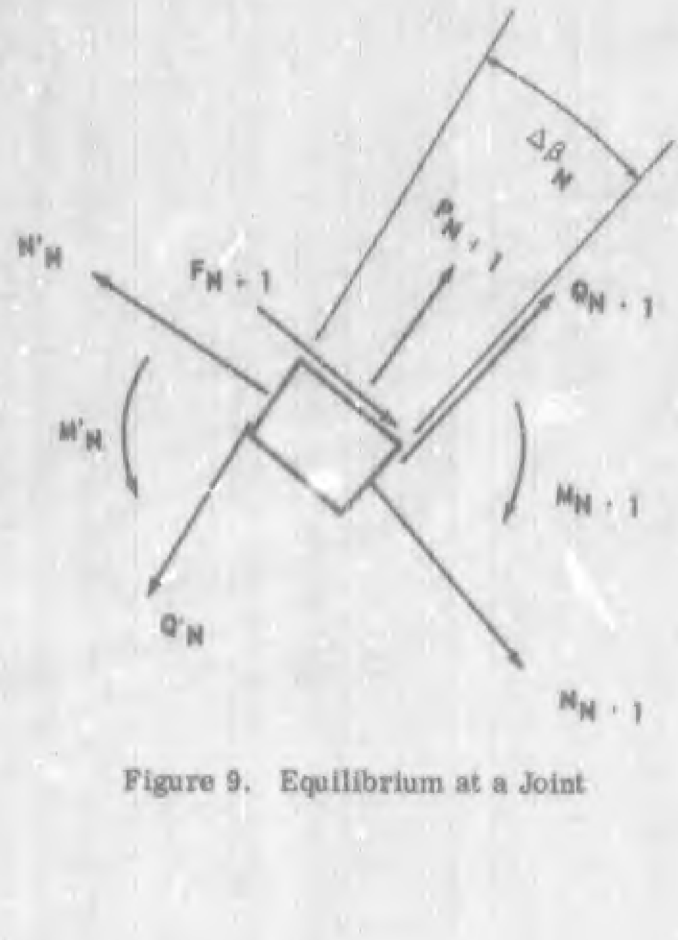

Figure 9. Equilibrium at a Joint

The primed quantities of eq. (14) can be eliminated by the use of eq. (13) and the following equations of equilibrium are obtained:

$$n_{N+1} - n_N \left(\cos \Delta\phi_N - \Delta\beta_N \sin \Delta\phi_N\right) + q_N \left(\sin \Delta\phi_N + \Delta\beta_N \cos \Delta\phi_N\right) = -f_{N+1} \tag{15a}$$

$$q_{N+1} - q_N \left(\cos \Delta\phi_N - \Delta\beta_N \sin \Delta\phi_N\right) - n_N \left(\sin \Delta\phi_N + \Delta\beta_N \cos \Delta\phi_N\right) = -p_{N+1} \tag{15b}$$

$$m_{N+1} - m_N - n_N \left(1 - \cos \Delta\phi_N\right) - q_N \sin \Delta\phi_N = 0. \tag{15c}$$

C. Constitutive Equations

The constitutive equations are those which relate the relative displacements and rotations of an element to the forces and moments acting onthe element.

The assumptions of the Winkler-Bach theory [3] of curved beams form the basis of this analysis. That is, a plane cross section of the arch remains plane and normal to the centroidal line and the deformation of the cross section is negligible when computing the extensional strain. This theory gives the following strain energy integral:

$$\gamma = \frac{R}{2EA} \int_0^{\Delta\phi_N} \left[\frac{1}{Z} \left(\frac{M_\alpha}{R}\right)^2 + \left(N_\alpha + \frac{M_\alpha}{R}\right)^2 \right] d\alpha. \tag{16}$$

From Figure 10,

$$\begin{aligned} N_\alpha &= N'_N \cos \alpha + Q'_N \sin \alpha \\ M_\alpha &= M'_N - Q'_N R \sin \alpha + N'_N R (1 - \cos \alpha). \end{aligned} \tag{17}$$

is obtained.

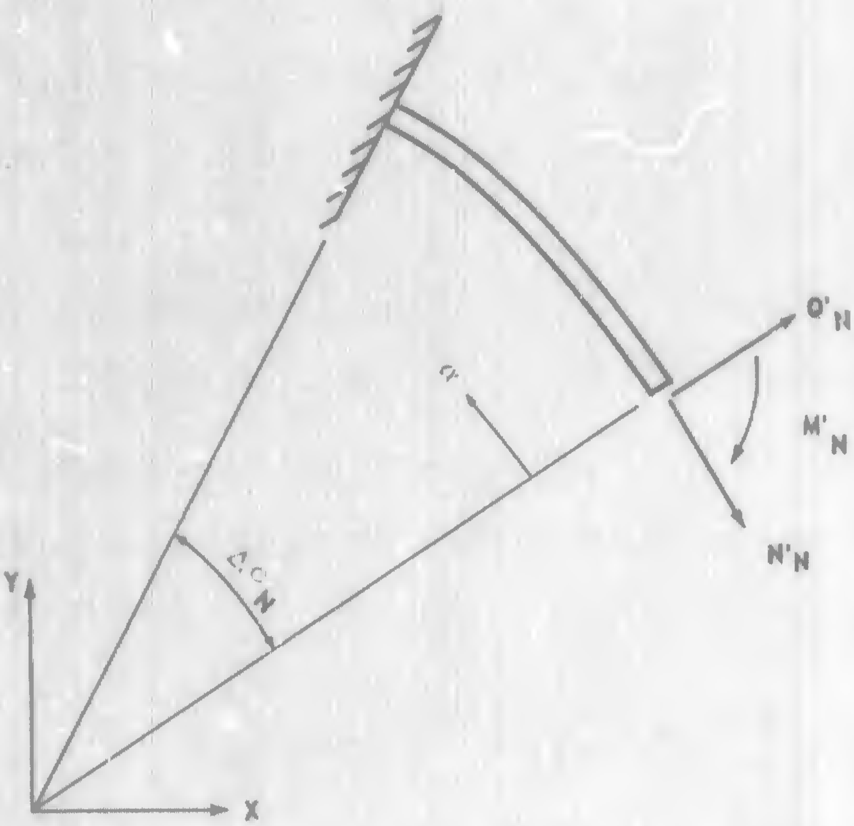

Figure 10. Constrained Element

The substitution of eq. (17) into the strain energy integral eq. (16) yields

$$\gamma = \frac{R}{2EA} \int_0^{\Delta\phi_N} \left\{ \frac{1}{Z} \left[\frac{M'_N}{R} - Q'_N \sin\alpha + N'_N (1 - \cos\alpha) \right]^2 + \left[\frac{M'_N}{R} + N'_N \right]^2 \right\} d\alpha. \tag{18}$$

Expanding and integrating,

$$\begin{aligned} \gamma = \frac{R}{2EA} \Bigg\{ \frac{1}{Z} \Bigg[& \frac{\overline{M'_N}^2}{R^2} \Delta\phi_N + \overline{Q'_N}^2 \left(\frac{\Delta\phi_N}{2} - \frac{\sin 2\Delta\phi_N}{4} \right) \\ & + \overline{N'_N}^2 \left(\frac{3\Delta\phi_N}{2} - 2\sin\Delta\phi_N + \frac{\sin 2\Delta\phi_N}{4} \right) - \frac{2M'_N Q'_N}{R} \left(1 - \cos\Delta\phi_N \right) \\ & + 2\frac{M'_N N'_N}{R} \left(\Delta\phi_N - \sin\Delta\phi_N \right) - 2Q'_N N'_N \Big(1 - \cos\Delta\phi_N \\ & - \frac{1}{2}\sin^2\Delta\phi_N \Big) \Bigg] + \left[\frac{\overline{M'_N}^2}{R^2}\Delta\phi_N + \frac{2M'_N N'_N}{R}\Delta\phi_N + \overline{N'_N}^2 \Delta\phi_N \right] \Bigg\} \end{aligned} \tag{19}$$

is obtained.

By the use of Castigliano's theorem of deflections and a corollary on rotations, we obtain the displacements and rotation components at the point of application of the forces N'_N and Q'_N and the moment M'_N respectively. In general, a generalized displacement q_i caused by a generalized external load F_i is given by

$$q_i = \frac{\partial\gamma}{\partial F_i} .$$

Applying this relation to eq. (19), we obtain

$$\Delta U_N = \frac{\partial \gamma}{\partial N'_N} = \frac{R}{EA}\left\{\frac{1}{Z}\left[N'_N\left(\frac{3\Delta\phi_N}{2} - 2\sin\Delta\phi_N + \frac{1}{4}\sin 2\Delta\phi_N\right)\right.\right.$$

$$\left. + \frac{M'_N}{R}\left(\Delta\phi_N - \sin\Delta\phi_N\right) - Q'_N\left(1 - \cos\Delta\phi_N - \frac{1}{2}\sin^2\Delta\phi_N\right)\right]$$

$$\left. + \frac{M'_N}{R}\Delta\phi_N + N'_N\Delta\phi_N\right\}. \qquad (20)$$

Using the nondimensional relations of eq. (11), we obtain the nondimensional equation

$$\Delta u_N \equiv \frac{\Delta U_N}{R\Delta\phi_N} = n'_N\left[Z + \frac{1}{\Delta\phi_N}\left(\frac{3}{2}\Delta\phi_N - 2\sin\Delta\phi_N + \frac{1}{4}\sin 2\Delta\phi_N\right)\right]$$

$$+ m'_N\left[Z + \frac{1}{\Delta\phi_N}\left(\Delta\phi_N - \sin\Delta\phi_N\right)\right] - \frac{q'_N}{\Delta\phi_N}\left[1 - \cos\Delta\phi_N\right.$$

$$\left. - \frac{1}{2}\sin^2\Delta\phi_N\right]. \qquad (21)$$

It is desired to have the constitutive equations in terms of the forces and moment at the left end of the element. Therefore, by the use of eq. (13), we arrive at the constitutive equation for the nondimensional relative displacement of the element in terms of the forces and moments at the left end of the element

$$\Delta u_N = n_N\left[Z + 1 - \frac{3}{2\Delta\phi_N}\sin\Delta\phi_N + \frac{1}{2}\cos\Delta\phi_N\right]$$

$$+ q_N\left[\frac{1}{\Delta\phi_N} - \frac{1}{2}\sin\Delta\phi_N - \frac{1}{\Delta\phi_N}\cos\Delta\phi_N\right] \qquad (22)$$

$$+ m_N\left[Z + \frac{1}{\Delta\phi_N}\left(\Delta\phi_N - \sin\Delta\phi_N\right)\right].$$

In a similar manner we obtain the nondimensional radial displacement Δv_N and relative rotation $\Delta\beta_N$ of the element

$$\Delta v_N \equiv \frac{\Delta V_N}{R\Delta\phi_N} = -\frac{1}{\Delta\phi_N}\left\{ n_N \left(\frac{\Delta\phi_N}{2} \sin\Delta\phi_N - 1 + \cos\Delta\phi_N \right) \right.$$

$$\left. - m_N (1 - \cos\Delta\phi_N) + q_N \left[\frac{1}{2} \left(\Delta\phi_N \cos\Delta\phi_N - \sin\Delta\phi_N \right) \right] \right\} . \qquad (23)$$

$$\Delta\beta_N = \Delta\phi_N \left[n_N \left(1 + Z - \frac{1}{\Delta\phi_N} \sin\Delta\phi_N \right) + m_N (1 + Z) \right.$$

$$\left. + \frac{q_N}{\Delta\phi_N} (1 - \cos\Delta\phi_N) \right] . \qquad (24)$$

These constitutive equations can be written in a more compact form as follows:

$$\Delta u_N = a_N n_N + b_N m_N + c_N q_N$$

$$\Delta v_N = d_N n_N + e_N m_N + f_N q_N \qquad (25)$$

$$\frac{\Delta\beta_N}{\Delta\phi_N} = g_N n_N + h_N m_N + i_N q_N ,$$

where

$$a_N = Z + 1 - \frac{3}{2\Delta\phi_N} \sin\Delta\phi_N + \frac{1}{2} \cos\Delta\phi_N$$

$$b_N = Z + 1 - \frac{1}{\Delta\phi_N} \sin\Delta\phi_N$$

$$c_N = \frac{1}{\Delta\phi_N} \left(1 - \cos\Delta\phi_N - \frac{1}{2} \Delta\phi_N \sin\Delta\phi_N \right) \qquad (26)$$

$$d_N = c_N$$

$$e_N = \frac{1}{\Delta_N}\left(1 - \cos \Delta\phi_N\right)$$

$$f_N = \frac{1}{2\Delta\phi_N}\left(\sin \Delta\phi_N - \Delta\phi_N \cos \Delta\phi_N\right)$$

$$g_N = b_N \qquad (26)$$

$$h_N = 1 + Z$$

$$i_N = e_N.$$

If the angle subtended by each of the elements is equal, then the coefficients of eq. (26) are the same for each of the links.

D. Boundary Conditions

Additional conditions are needed to achieve continuity at the apex and fulfillment of end conditions.

From Figure 11, we can write the continuity conditions at the apex. Signifying quantities to the right by a subscript +1 and to the left by a subscript -1, we obtain

$$M_{+1} = M_{-1}$$

$$\beta_{+1} = -\beta_{-1}$$

$$Q_{+1} + Q_{-1} = P \cos(\beta_1 + \rho)$$

$$N_{+1} - N_{-1} = -P \sin(\beta_1 + \rho)$$

These can be written in the nondimensional form by eq. (11)

$$\begin{aligned} m_{+1} &= m_{-1} \\ \beta_{+1} &= -\beta_{-1} \\ q_{+1} + q_{-1} &= p \cos(\beta_1 + \rho) \\ n_{+1} - n_{-1} &= -p \sin(\beta_1 + \rho) \end{aligned} \tag{27}$$

where ρ is the angle of incidence of the applied load P.

If the ends of the arch are restrained from a vertical and/or horizontal movement, then the relative displacement of these ends is zero, i.e.,

$$-\sum_{-N=-M}^{1} \Delta\overline{V}_N + \sum_{1}^{N=M} \Delta\overline{V}_N = 0 \tag{28}$$

At the ends of the arch, we consider two possibilities as to their fixity.

1. <u>Pinned Ends</u>. The condition for a pinned end requires the moment at that point M to vanish.

$$m_M = 0 \tag{29}$$

2. <u>Fixed Ends</u>. The condition for a fixed or built-in edge is that a tangent to the deflected middle surface coincide with the initial position of the middle line of the arch. This can be accomplished by setting the rotation β_M at point M equal to zero.

$$\beta_M = 0 \tag{30}$$

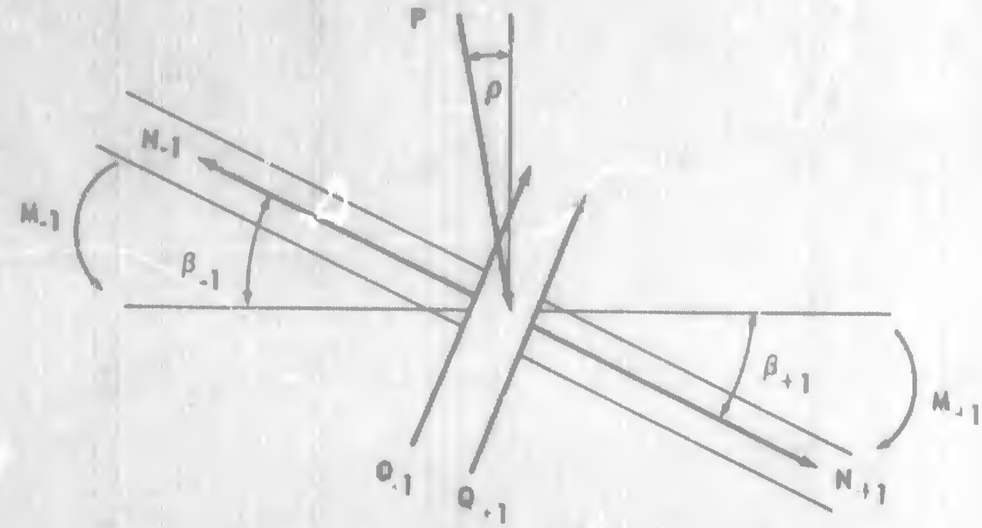

Figure 11. Equilibrium at Apex

CHAPTER III

SOLUTIONS TO THE NONLINEAR EQUATIONS BY THE METHOD OF INCREMENTAL LOADING

A. Concept

The equations developed in Chapter II are applicable to the arch for arbitrarily large deflections. A solution of these nonlinear equations becomes a formidable task unless some appropriate procedure is used.

The procedure presented here consists of linearizing only in terms of small changes of each variable. The approach is to allow the variables, tensions, shears, and rotations, to take on small changes corresponding to a small increase in load. For conciseness, let the nonlinear governing equations be represented by

$$F\left(x_i, P\right) = 0,$$

where x_i are the interelement tension forces, shear forces, and rotations due to the applied load P. By giving the variables $\left(x_i, P\right)$ a small increment $\left(\delta x_i, \delta P\right)$, the increment in F corresponding to the increments δx_i and δP is

$$\Delta F = \frac{\partial F}{\partial x_i} \delta x_i + \frac{\partial F}{\partial P} \delta P + \ldots,$$

where the derivatives are evaluated in the reference state.

If the system is in equilibrium, any increment of the variables must also satisfy equilibrium. Consequently,

$$\Delta F = 0 = \frac{\partial F}{\partial x_i} \delta x_i + \frac{\partial F}{\partial P} \delta P,$$

or in matrix form

$$\left[\frac{\partial F}{\partial x_i}\right] \left\{\delta x_i\right\} = \left\{- \frac{\partial F}{\partial P} \delta P\right\}. \qquad (31)$$

The variables δx_i can be computed for any prescribed nonzero increment δP since the coefficient matrix $\left[\frac{\partial F}{\partial x_i}\right]$ is a linear combination of the variables $\overline{x}_i$ and $\overline{P}$, where $\overline{P}$ is the sum of the preceding increments of δP's and $\overline{x}_i$ is the sum of the preceding δx_i's corresponding to the increments of δP.

The values $\overline{x}_i$ corresponding to $\overline{P}$ computed by eq. (31) do not satisfy the nonlinear equations $F\left(x_i, P\right) = 0$; i.e., $\overline{F}\left(\overline{x}_i, \overline{P}\right) \neq 0$, because only the first order terms were considered in the expansion of ΔF. A better approximation of the solution to the nonlinear equations is obtained if we examine further the Taylor series expansion of $F\left(x_i, P\right)$.

$$F\left(x_i, P\right) = \overline{F}\left(\overline{x}_i, \overline{P}\right) + \frac{\partial F}{\partial x_i} \delta x_i' + \frac{\partial F}{\partial P} \delta P' = 0.$$

The derivatives and $\overline{F}\left(\overline{x}_i, \overline{P}\right)$ are evaluated for the existing conditions $\overline{x}_i$ and $\overline{P}$. By setting the load increment $\delta P'$ equal to zero, the values $\delta x_i'$ needed to satisfy the condition

$$\overline{F}\left(\overline{x}_i, \overline{P}\right) + \frac{\partial F}{\partial x_i} \delta x_i' = 0$$

can be determined.

Therefore,

$$\frac{\partial F}{\partial x_i}\,\delta x_i' = -\,\overline{F}\left(\overline{x}_i,\,\overline{P}\right),$$

or in matrix form

$$\left[\frac{\partial F}{\partial x_i}\right]\left\{\delta x_i'\right\} = -\left[\overline{F}\left(\overline{x}_i,\,\overline{P}\right)\right]. \tag{32}$$

By summing these increments $\delta x_i'$ and $\delta P' = 0$ with the previous solutions $\overline{x}_i$ and $\overline{P}$ we obtain a better solution to the equations

$$F\left(x_i,\,P\right) = 0. \tag{33}$$

The corrected solution is thus given by

$$x_i^* = \overline{x}_i + \delta x_i' \tag{34}$$

and

$$P^* = \overline{P} = \sum \delta P. \tag{35}$$

Thus, by eq. (31) we obtain an approximate solution for a prescribed load increment and by eq. (32) we obtain the corrected increments for a better solution to the nonlinear equations.

When the structure reaches the branch point, the determinant $\left[\frac{\delta F}{\partial x_i}\right]$ of the coefficients $\left\{\delta x_i\right\}$ vanishes. At this branch point, the important question of stability must be answered. This question can be answered by rearranging the equations so that an incremental vertical displacement can be prescribed and observing the path that the arch follows as described in Chapter I.

B. Derivation of Linear Equations

Introducing the following nondimensional quantities as before,

$$\Delta v_N = \frac{\Delta V_N}{R\Delta\phi_N} \qquad \Delta u_N = \frac{\Delta U_N}{R\Delta\phi_N} \tag{36}$$

$$\Delta x_N = \frac{\Delta X_N}{R\Delta\phi_N} \qquad \Delta y_N = \frac{\Delta Y_N}{R\Delta\phi_N} \ ,$$

and neglecting the small terms of eq. (10) we obtain the incremental kinematical relations

$$\delta x_N = \pm \left\{ \left[-\frac{2}{\Delta\phi_N} \sin\left(\frac{\Delta\phi_N}{2}\right) \sin\left(\phi_{N1/2} + \psi^*_N\right) \right] \delta\psi_N + \delta u_N \cos\left(\phi_{N+1} + \psi^*_N\right) - \delta v_N \sin\left(\phi_{N+1} + \psi^*_N\right) \right\} \tag{37a}$$

$$\delta y_N = - \left\{ \left[\frac{2}{\Delta\phi_N} \sin\left(\frac{\Delta\phi_N}{2}\right) \cos\left(\phi_{N1/2} + \psi^*_N\right) \right] \delta\psi_N + \delta u_N \sin\left(\phi_{N+1} + \psi^*_N\right) + \delta v_N \cos\left(\phi_{N+1} + \psi^*_N\right) \right\} \tag{37b}$$

These are the incremental kinematical relationships for each of the elements in the arch.

The equilibrium eq. (15) become

$$\delta n_{N+1} - A_N\,\delta n_N + C_N\,\delta q_N + \left(n^*_N \sin\Delta\phi_N + q^*_N \cos\Delta\phi_N\right)\delta\left(\Delta\psi_N\right) = -\,\delta f_{N+1} \tag{38a}$$

$$\delta q_{N+1} - A_N\,\delta q_N - C_N\,\delta n_N + \left(q^*_N \sin\Delta\phi_N - n^*_N \cos\Delta\phi_N\right)\delta\left(\Delta\psi_N\right) = -\,\delta p_{N+1} \tag{38b}$$

$$\delta m_{N+1} - \delta m_N - \delta n_N\left(1 - \cos\Delta\phi_N\right) - \delta q_N \sin\Delta\phi_N = 0, \tag{38c}$$

where

$$A_N = \cos \Delta\phi_N - \Delta\beta_N^* \sin \Delta\phi_N \tag{39a}$$

$$C_N = \sin \Delta\phi_N + \Delta\beta_N^* \cos \Delta\phi_N \tag{39b}$$

$$\Delta\beta_N = \beta_{N+1} - \beta_N \tag{39c}$$

$$\delta\left(\Delta\beta_N\right) = \delta\beta_{N+1} - \delta\beta_N , \tag{39d}$$

and the asterisked values are the sum of the previous increments.

From the constitutive relations, eq. (25), we obtain,

$$\delta u_N = a_N\, \delta n_N + b_N\, \delta m_N + c_N\, \delta q_N \tag{40a}$$

$$\delta v_N = d_N\, \delta n_N + e_N\, \delta m_N + f_N\, \delta q_N \tag{40b}$$

$$\frac{\delta\left(\Delta\beta_N\right)}{\Delta\phi_N} = g_N\, \delta n_N + h_N\, \delta m_N + i_N\, \delta q_N . \tag{40c}$$

From the boundary conditions, eq. (27), the incremental relationships at the apex are

$$\delta m_{+1} = \delta m_{-1} \tag{41a}$$

$$\delta\beta_{+1} = -\,\delta\beta_{-1} \tag{41b}$$

$$\delta q_{+1} + \delta q_{-1} + p^* \sin\left(\beta_1^* + \rho\right) \delta\beta_1 = \delta p \cos\left(\beta_1 + \rho\right) \tag{41c}$$

$$\delta n_{+1} - \delta n_{-1} + p^* \cos\left(\beta_1^* + \rho\right) \delta\beta_1 = \delta p \sin\left(\beta_1 + \rho\right) , \tag{41d}$$

and from eq. (28)

$$-\sum_{-N=-M}^{1} \delta\vec{V}_N + \sum_{1}^{N=M} \delta\vec{V}_N = 0. \tag{42}$$

The incremental equations for the boundaries at point M are

1. Pinned Ends

$$\delta m_M = 0.0 = \frac{1}{h_N}\left[\delta\left(\Delta\beta_N\right)/\Delta\phi_N - g_N\,\delta n_N - i_N\,\delta q_N\right] \tag{43}$$

2. Fixed Ends

$$\delta\beta_M = 0.0 \tag{44}$$

The problem is more conveniently solved if the governing equations are formulated in terms of the tension force n_N, the shear force q_N and the rotations β_N as previously noted. Thus, the kinematical relations of eq. (37) become

$$\begin{aligned}
\delta x_N = \pm \Bigg\{ & \Bigg[-2\sin\left(\frac{\Delta\phi_N}{2}\right)\sin\left(\phi_{N1/2}+\beta^*_N\right) - \frac{b_N}{h_N}\cos\left(\phi_{N+1}+\beta^*_N\right) \\
& + \frac{e_N}{h_N}\sin\left(\phi_{N+1}+\beta^*_N\right)\Bigg]\frac{\delta\beta_N}{\Delta\phi_N} + \Bigg[\frac{b_N}{h_N}\cos\left(\phi_{N+1}+\beta^*_N\right) \\
& - \frac{e_N}{h_N}\sin\left(\phi_{N+1}+\beta^*_N\right)\Bigg]\,\delta\beta_{N+1}/\Delta\phi_N \\
& + \Bigg[\left(a_N - \frac{g_N\,b_N}{h_N}\right)\cos\left(\phi_{N+1}+\beta^*_N\right) \\
& - \left(d_N - \frac{g_N\,e_N}{h_N}\right)\sin\left(\phi_{N+1}+\beta^*_N\right)\Bigg]\,\delta n_N \\
& + \Bigg[\left(c_N - \frac{i_N\,b_N}{h_N}\right)\cos\left(\phi_{N+1}+\beta^*_N\right) \\
& - \left(f_N - \frac{i_N\,e_N}{h_N}\right)\sin\left(\phi_{N+1}+\beta^*_N\right)\quad \delta q_N \Bigg\}
\end{aligned} \tag{45a}$$

$$\delta y_N = -\left\{\left[2\sin\left(\frac{\Delta\phi_N}{2}\right)\cos\left(\phi_{N1/2}+\beta^*_N\right) - \frac{b_N}{h_H}\sin\left(\phi_{N+1}+\beta^*_N\right)\right.\right.$$

$$\left. - \frac{e_N}{h_N}\cos\left(\phi_{N+1}+\beta^*_N\right)\right]\frac{\delta\beta_N}{\Delta\phi_N} + \left[\frac{b_N}{h_N}\sin\left(\phi_{N+1}+\beta^*_N\right)\right.$$

$$\left. + \frac{e_N}{h_N}\cos\left(\phi_{N+1}+\beta^*_N\right)\right]\delta\beta_{N+1}/\Delta\phi_N$$

$$+\left[\left(a_N - \frac{g_N b_N}{h_N}\right)\sin\left(\phi_{N+1}+\beta^*_N\right)\right. \tag{45b}$$

$$\left. + \left(d_N - \frac{g_N e_N}{h_N}\right)\cos\left(\phi_{N+1}+\beta^*_N\right)\right]\delta n_N$$

$$+\left[\left(c_N - \frac{i_N b_N}{h_N}\right)\sin\left(\phi_{N+1}+\beta^*_N\right)\right.$$

$$\left.\left. + \left(f_N - \frac{i_N e_N}{h_N}\right)\cos\left(\phi_{N+1}+\beta^*_N\right)\right]\delta q_N\right\} .$$

Similarly, the equilibrium eq. (38) are

$$\delta n_{N+1} - A_N\,\delta n_N + C_N\,\delta q_N + \left(n^*_N\sin\Delta\phi_N + q^*_N\cos\Delta\phi_N\right)\delta\left(\Delta\beta_N\right)$$
$$= -\,\delta f_{N+1} \tag{46a}$$

$$\delta q_{N+1} - A_N\,\delta q_N - C_N\,\delta n_N + \left(q^*_N\sin\Delta\phi_N - n^*_N\cos\Delta\phi_N\right)\delta\left(\Delta\beta_N\right)$$
$$= -\delta p_{N+1} \tag{46b}$$

$$\left(\delta\beta_{N+2} - 2\,\delta\beta_{N+1} + \delta\beta_N\right)\Big/\left(h_N\,\Delta\phi_N\right) - \frac{g_N}{h_N}\,\delta n_{N+1} - \frac{i_N}{h_N}\,\delta q_{N+1}$$
$$- \delta n_N\left(1 - \cos\Delta\phi_N - \frac{g_N}{h_N}\right) - \delta q_N\left(\sin\Delta\phi_N - \frac{i_N}{h_N}\right) = 0.0 \tag{46c}$$

Equations (46) contain seven unknowns per link. Thus, 3 equations per link = 8 remaining equations needed for a solution. These eight equations are the boundary eq. (41) and (42) and a set of end conditions (43) or (44) depending upon the type of fixity at the ends. These are the governing equations for the incremental deformation of the arch. They are linear in the unknowns δn_N, δq_N and $\delta\beta_N$. Notice that the increment in load (δP) only appears in eq. (41). These linear equations are easily solved on a large digital computer and, with the correction procedure noted herein, the variables are corrected so as to satisfy the nonlinear equations.

C. Computation

The computational procedure for the solution of an arch with concentrated vertical central load is as follows:

1) The incremental vertical load (δP) is set to a small value.

2) All terms with an asterisk are set equal to zero.

3) The system of equations is solved to determine the initial incremental values $\left(\delta x_i\text{'s}\right)$.

4) The incremental values of step 3) are added to the previous asterisked values.

5) The value of the determinant and the vertical displacement under the load is retained.

6) The load increment is set equal to zero.

7) The asterisked quantities $\left(n^*_N, q^*_N, \beta^*_N\right)$ are required to satisfy the nonlinear equations. The corrective increments $\left(\delta x'_i\right)$ are computed according to eq. (32).

8) These values $\left(\delta x'_i\right)$ are added to the asterisked values.

9) A new load increment is added.

10) Steps 3) through 9) are repeated until the determinant vanishes or until the increment in vertical displacement exceeds by 10 percent the total vertical displacement.

11) The equations are rearranged so that an increment of vertical displacement is now specified

12) The equations are solved and the resulting increments $\left(\delta x_i\right)$ are added to the asterisked values.

13) Successive increments in vertical displacement can be used to carry the structure to its deformed post buckled state.

The results of this computational procedure are presented in Chapter IV.

CHAPTER IV

CONCLUSIONS

The equations that have been developed were programmed on the IBM 7094 computer. Three arches subjected to a concentrated vertical force p were studied: First, a semi-circular arch with pinned ends is studied from the unloaded position to a point where significant side sway developed (Figure 12). This work is compared with that done by Langhaar, Boresi and Carver [4]. Secondly a shallow arch with fixed ends (Figure 13), is studied from the unloaded position to a point past snap through. This work is compared with that done by Schreyer and Masur [5]. Finally, an arch which has the height to radius ratio of one-half ($H/R = 0.5$) was studied and compared with the work of Huddleston [6].

The results of the semi-circular arch analysis are presented in Figure 13. The bifurcation point was found to be

$$P_{cr} = 6.17\ EAZ.$$

The work done by Langhaar, et al., yields the critical load of

$$P_{cr} = 6.54\ EAZ.$$

This is a decrease of 5.7 percent in the critical load. This decrease can be attributed to the consideration of the extension of the centroidal axis and the pre-buckled deformations.

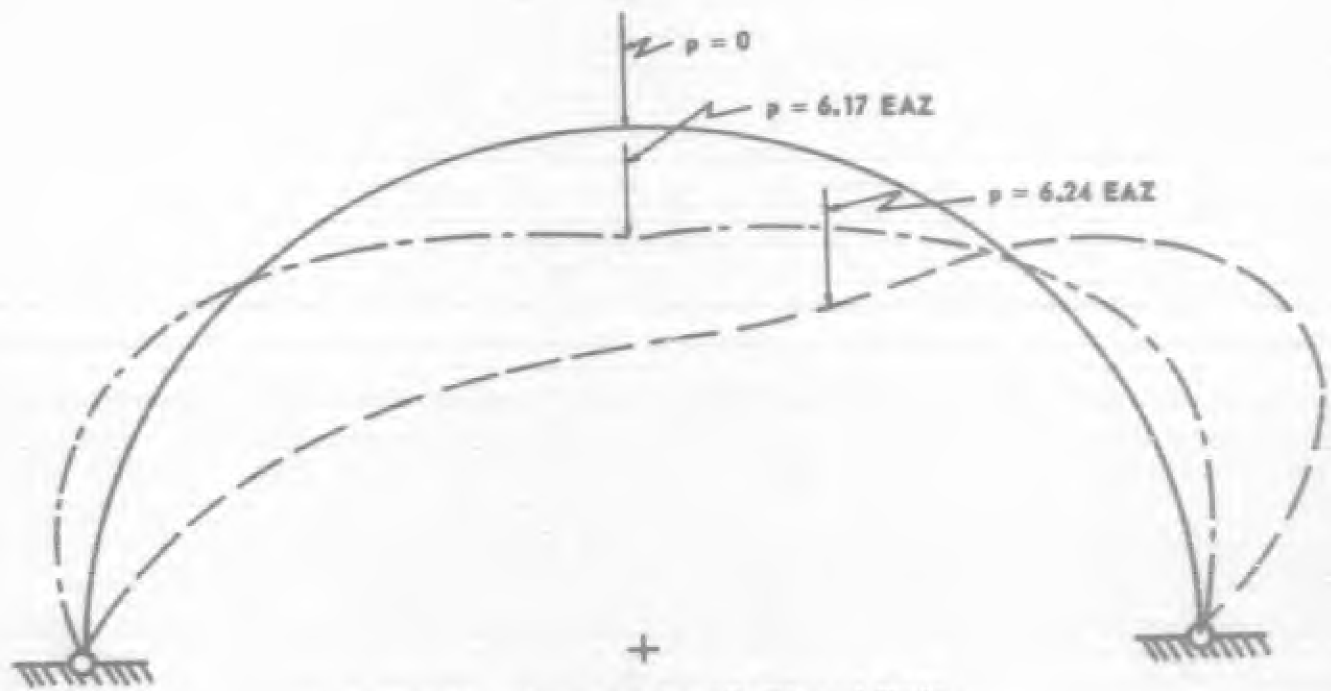

Figure 12. Steep Arch with Pinned Ends

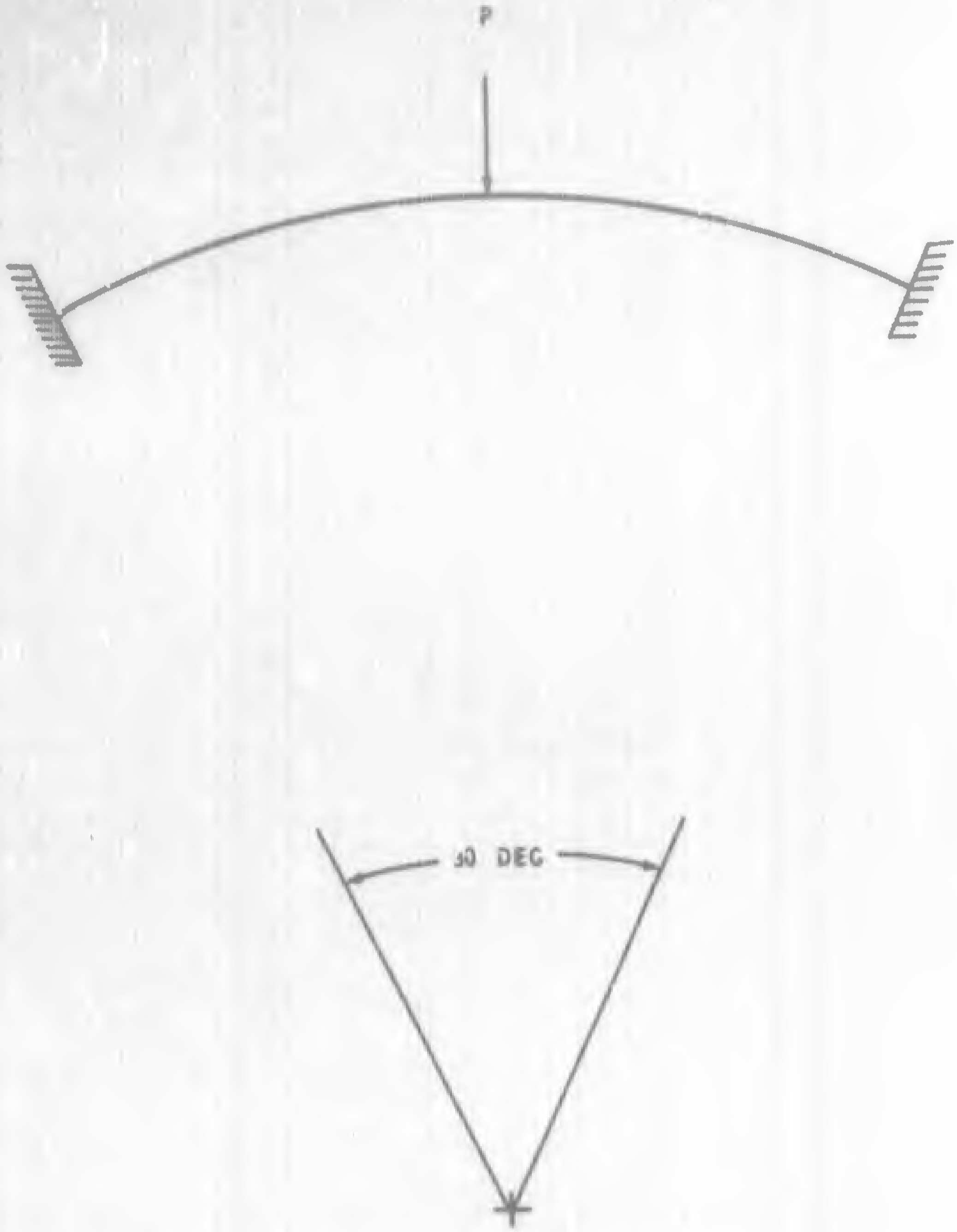

Figure 13. Shallow Arch with Fixed Ends

The experimental results performed by Langhaar, et al., show that the arch develops side sway at a load of approximately 3.70 pounds. However, the results of the finite element analysis shows no side sway until the bifurcation point is reached at approximately 3.98 pounds. It is likely that the side sway developed prematurely in the experiment because of a non-symmetry in the arch or load. It has been found from the computer program that a small deviation from vertical application of the load causes the arch to sway before the critical load is reached. This is shown in Figure 14 as the dotted line for a load 0.001 degrees from vertical.

The corrected theoretical buckling loads given by Langhaar, et al., agree with those computed by the finite element method and incremental loading; however, mass was not considered in this analysis.

The shallow arch that was investigated corresponds with an example presented by Schreyer, et al. This example is identified by a geometric parameter λ equal to 25, where

$$\lambda \cong \frac{2H}{h} ,$$

H is the rise of the arch and h is the thickness. For a 30 degree arch considered in this work, Schreyer and Masur give snap through at a load of

$$P = (57.+)\ EAZ.$$

The finite element analysis gives this value as

$$P = 57.1\ EAZ.$$

The analysis predicted no bifurcation point between the unloaded and the snap through point (Figure 15). This corresponds with the results of

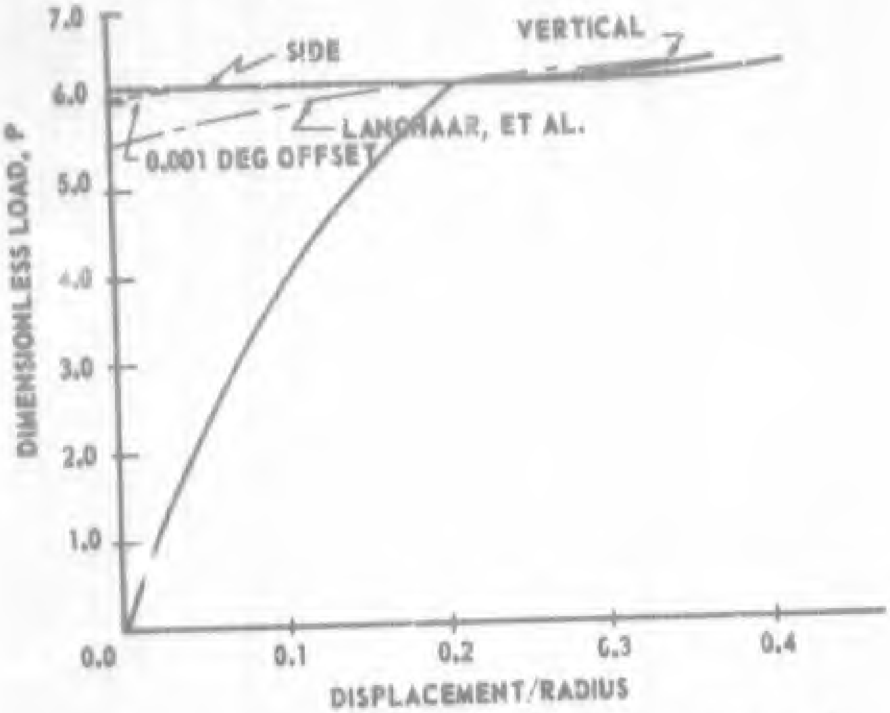

Figure 14. Load Versus Displacement of a Steep Arch

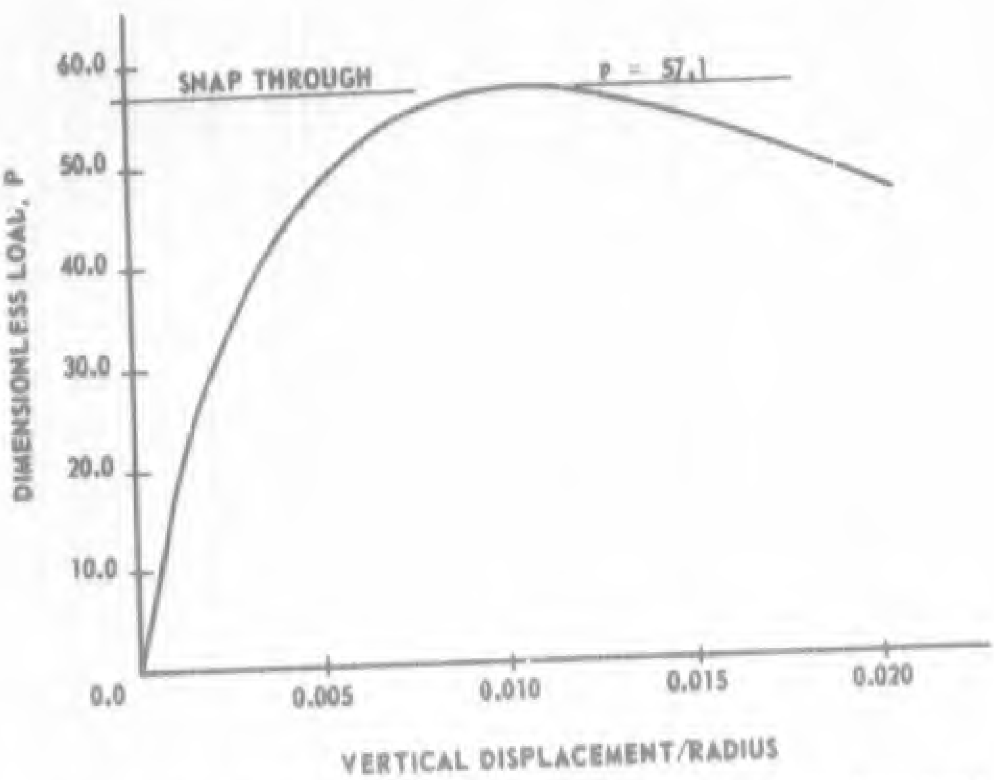

Figure 15. Load Versus Vertical Displacement of a Shallow Arch

Schreyer and Masur; however, the latter predict a bifurcation point later in the load-displacement curve. The finite element analysis was not carried far enough to determine this point or if it existed.

The intermediate steep arch where $H/R = 0.5$, a critical load $P_{cr} = 12.74$ was computed. For an "incompressible" arch, Huddleston [6] obtained $P_{cr} = 12.9$, as closely as we can read his curve. Our computation shows, too, that the critical state is unstable, i.e., snap-through ensues.

The results presented here indicate that the methods described provide a useful tool for predicting the response of arches, including the influence of eccentricities.

There appear to be no difficulties in extending the procedures to arches of other shapes and nonuniform cross sections. Slight variations of curvature can be treated by the Winkler-Bach theory. Rapidly varying properties can be handled by other approximations for the individual elements. Imperfections can be included by modifications of the equations governing individual elements.

The technique of incremental loading is also a natural way to treat inelastic elements and so to predict progressive yielding and collapse of arches and shells. Equations (25) must be replaced by linear equations governing plastic and elastic increments and augmented by yield criteria.

REFERENCES

1. J. T. Oden and G. A. Wempner, Numerical Analysis of Arbitrary Shell Structures under Arbitrary Static Loadings, UARI Research Report No. 47, November 1967.

2. R. A. Toupin, "The Elastic Dielectric," J. Rational Mech. Anal., Vol. 5, N. 6, 1956, pp. 849-914.

3. Fred B. Seely, Resistance of Materials, New York, John Wiley and Sons, Inc., 1955, p. 366.

4. H. L. Langhaar, A. P. Boresi, and D. R. Carver, "Energy Theory of Buckling of Circular Elastic Rings," Proceedings of the Second U. S. National Congress of Applied Mechanics, June 1954.

5. H. L. Schreyer and E. F. Masur, "Buckling of Shallow Arches," Journal of the Engineering Mechanics Division, ASCE, No. EM4, Paper 4875, August 1966, pp. 1-19.

6. J. V. Huddleston, "Finite Deflections and Snap-Through of High Circular Arches," Journal of Applied Mechanics, preprint 68-WA/APM 18.

7. G. Wempner, "Finite Elements, Finite Rotations and Small Strain of Flexible Shells," Int. J. Solids and Structures, Vol. 3, 1968.

BIBLIOGRAPHY

1. H. L. Langhaar, Energy Methods in Applied Mechanics, New York, John Wiley and Sons, Inc., 1962, pp. 75-103.

2. F. B. Hildebrand, Introduction to Numerical Analysis, New York, McGraw-Hill Book Company, Inc., 1956.

3. Y. C. Fung and A. Kaplan, Buckling of Low Arches or Curved Beams of Small Curvature, NACA TN 2840, November 1952.

4. A. Gjelsvik and S. R. Bodner, "The Energy Criterion and Snap Buckling of Arches," Journal of the Engineering Mechanics Division, ASCE, No. EM5, October 1962, pp. 87-134.

5. G. A. Wempner and N. E. Kesti, "Buckling of Circular Arches and Rings," 4th Math. Congress of Applied Mechanics, 1962, pp. 843-849.

6. G. A. Wempner and T. Ewbank, "Buckling of Circular Arches Under Nonuniform Pressure," J. Eng. Mech. Div. ASCE 3597, EM4, 1963, pp. 17-20.

UNCLASSIFIED

Security Classification

DOCUMENT CONTROL DATA - R & D

(Security classification of title, body of abstract and indexing annotation must be entered when the overall report is classified)

1. ORIGINATING ACTIVITY (Corporate author) Structures and Mechanics Laboratory Research and Development Directorate U.S. Army Missile Command Redstone Arsenal, Alabama 35809	2a. REPORT SECURITY CLASSIFICATION Unclassified 2b. GROUP N/A

3. REPORT TITLE

NUMERICAL METHODS FOR THE NONLINEAR ANALYSIS OF AN ELASTIC ARCH

4. DESCRIPTIVE NOTES (Type of report and inclusive dates)

None

5. AUTHOR(S) (First name, middle initial, last name)

Grady E. Patrick, Jr.

6. REPORT DATE	7a. TOTAL NO. OF PAGES	7b. NO. OF REFS
9 December 1968	51	7

8a. CONTRACT OR GRANT NO.	9a. ORIGINATOR'S REPORT NUMBER(S)
b. PROJECT NO. (DA) 1L013001A91A	RS-TR-68-15
c. AMC Management Structure Code No. 5016.11.84400.60 d.	9b. OTHER REPORT NO(S) (Any other numbers that may be assigned this report) AD________

10. DISTRIBUTION STATEMENT

This document is subject to special export controls and each transmittal to foreign governments or foreign nationals may be made only with prior approval of this Command, ATTN: AMSMI-RS.

11. SUPPLEMENTARY NOTES	12. SPONSORING MILITARY ACTIVITY
None	Same as No. 1

13. ABSTRACT

In a recent paper, Wempner presented a method by which the finite deflections of thin shells are approximated in finite elements and the nonlinear differential equations are replaced by nonlinear algebraic equations. This is accomplished by decomposing the motion of an element into a rigid-body rotation and a deformation. The deformation of a Hookean element is characterized by linear constitutive equations relating generalized forces and small relative displacements. Nonlinearities arise from the differences in the rigid-body rotations of adjacent elements.

In the present paper, the method is applied to formulate algebraic equations for the finite deflections of a circular arch. The constitutive equations of the finite element are the exact linear equations of the Winkler-Bach theory.

The nonlinear algebraic equations are replaced by a succession of linear equations, each governing the response to a small increment of load. To eliminate cumulative error, the numerical results are inserted in the nonlinear equations and corrected by the Newton-Raphson procedure.

DD FORM 1 NOV 65 1473 REPLACES DD FORM 1473, 1 JAN 64, WHICH IS OBSOLETE FOR ARMY USE.

UNCLASSIFIED

Security Classification

14. KEY WORDS	LINK A		LINK B		LINK C	
	ROLE	WT	ROLE	WT	ROLE	WT
Finite deflections						
Nonlinear differential equations						
Nonlinear algebraic equations						
Nonlinear analysis of elastic arch						
Rigid-body rotation						
Deformation of Hookean element						
Algebraic equations -Finite deflections of circular arch						
Winkler-Bach theory						
Newton-Raphson procedure						